Hydrodynamic coefficients induced by waves and currents for submerged circular cylinder

Yong Li, Mian Lin*

Lab. of Environmental Mechanics,Institute of Mechanics, Chinese Academy of Sciences, Beijing 100190, China

Abstract

Hydrodynamic coefficients induced by waves and currents are simulated for a stationary submerged circular cylinder in a two-dimensional numerical wave-current tank. In present paper, based on the Reynolds averaged Navier-Stokes equations, a two-dimensional numerical tank is developed to simulate the coaction processes. The computational vertical distributions of time-average velocity agree well with the experimental data, which indicates that the wave-current numerical tank has a good characteristic of wave-current combined flow. By using time histories of wave force, drift force are calculated. The computational results are also shown to be in good agreement with experimental and numerical results of other researchers. Simulated wave forces are employed to derive drag and inertia coefficients by using least-squares method. The coefficients induced by waves and wave-current flows are compared. The results indicate that the currents have a significant influence on the drag coefficients for submerged circular cylinder.

1. Introduction

In the lake area, waves commonly propagate on currents. The interaction of waves and currents affects the response of submerged structures, which must be considered in the design. It is of increasing important to precisely estimate the hydrodynamic forces and coefficients induced by waves and currents for Archimedes Bridge (AB), which belonged to the category of submerged floating tunnel.

Until now, there are many studies about the hydrodynamic forces and coefficients induced by waves for submerged objects, such as Vinje and Brevig [1], Clement and Mas [2], Venugopal et al. [3], and so on, while not many studies under wave-current flows have been conducted. In order to achieve a better understanding of the fluid mechanics in wave-current flows and loads on submerged cylinders, laboratory and computational studies are essential. Venugopal et al. [4] measured drag and inertia coefficients for horizontally submerged rectangular cylinders in waves and currents. For computational studies about waves, the numerical wave tank is often

---

* Corresponding author. Tel.: +86-10-8254-4206.
E-mail address: liyong@imech.ac.cn

mentioned, but the traditional numerical wave tank usually can not be used to simulate the wave and current combined flow (Koo and Kim [5], Dong and Zhan [6], etc).

In present paper, a two-dimensional numerical tank is developed to simulate the coaction processes. The wave-current tank is mainly based on the Reynolds averaged Navier-Stokes equations (RANS) equations and the model is used to simulate the turbulence. The equations are discretized based on the finite volume method (FVM) and the pressure implicit splitting of operators (PISO) scheme is employed to solve the Navier–Stokes equations.

1.1. Mathematical formulation

The governing equations are the RANS equations.

$$\frac{\partial \rho}{\partial t} + \frac{\partial}{\partial x_j}\left(\rho u_j\right) = 0 \tag{1}$$

$$\frac{\partial}{\partial t}\left(\rho u_i\right) + \frac{\partial}{\partial x_j}\left(\rho u_j u_i\right) = -\frac{\partial p}{\partial x_i} + \frac{\partial}{\partial x_j}\left[\mu_e\left(\frac{\partial u_j}{\partial u_i} + \frac{\partial u_i}{\partial u_j}\right)\right] + \rho g_i \tag{2}$$

where x_j ($j = 1, 2, 3$) represents the coordinate components, u_j is the fluid velocity, p is pressure, ρ is the density, g is the acceleration of gravity. $\mu_e = \mu + \mu_f$, μ is the fluid viscosity, $\mu = 1.002 \times 10^{-6}$ m²/s, μ_f is the turbulent eddy viscosity, $\mu_f = C_\mu \rho k^2 / \varepsilon$. k is turbulent kinetic energy, ε is turbulent energy dissipation rate.

The $k - \varepsilon$ two-equation model is adopted to estimate the turbulence.

$$\frac{\partial}{\partial t}\left(\rho k\right) + \frac{\partial}{\partial x_j}\left(\rho u_j k\right) = \frac{\partial}{\partial x_j}\left[\left(\mu + \frac{\mu_f}{\delta_k}\right)\frac{\partial k}{\partial x_j}\right] + P_k - \rho\varepsilon \tag{3}$$

$$\frac{\partial}{\partial t}\left(\rho\varepsilon\right) + \frac{\partial}{\partial x_j}\left(\rho u_j \varepsilon\right) = \frac{\partial}{\partial x_j}\left[\left(\mu + \frac{\mu_f}{\delta_\varepsilon}\right)\frac{\partial \varepsilon}{\partial x_j}\right] + C_1 P_k \frac{\varepsilon}{k} - C_2 \rho\frac{\varepsilon^2}{k} \tag{4}$$

$$P_k = \mu_f\left(\frac{\partial u_i}{\partial u_j} + \frac{\partial u_j}{\partial u_i}\right)\frac{\partial u_i}{\partial u_j} \tag{5}$$

where δ_k and δ_ε are the turbulent Schmidt numbers, the values of constants for above equations are given as follows: $C_\mu = 0.09$, $C_1 = 1.44$, $C_2 = 1.92$, $\delta_k = 1.0$, $\delta_\varepsilon = 1.33$.

In order to capture the water-air free surface, an Eulerian method named the volume of fluid (VOF) method is adopted. The equation for the volume fraction is:

$$\frac{\partial \alpha}{\partial t} + \frac{\partial}{\partial x_j}\left(u_j \alpha\right) = 0 \tag{6}$$

where α is the volume fraction of water and $1-\alpha$ represents the volume fraction of air. Volume fraction of each liquid is used as the weighting factor to get the mixture properties, such as density and viscosity, i.e.

$$\rho = \alpha\rho_w + (1 - \alpha)\rho_a \tag{7}$$

where ρ_w and ρ_a represent the density of water and air respectively.

1.2. Boundary

The entire computational domain with bottom topography is shown in Fig.1 , where d is the water depth, h is the centre of the test section from the still water level (SWL), and there are basically five boundary types associated with the governing equation: inlet, outlet, structure wall, bed, and atmosphere.
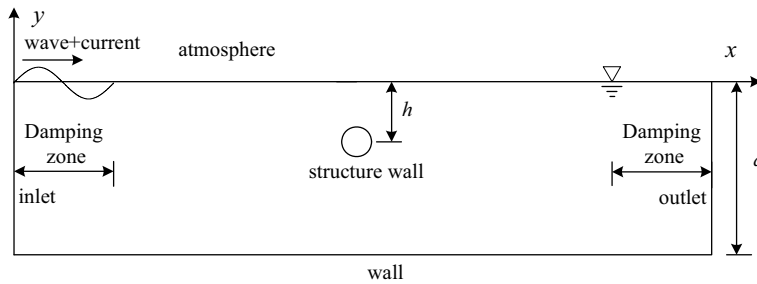

Fig. 1. Comparison of drift force

Boundary conditions associated with waves and currents are prescribed along the inlet of computational domain. The pressure and turbulence quantities including k and ε are set to be zero normal gradient and the velocity vector is specified by Stokes regular waves and current. The theoretical velocity combined waves with currents can be expressed by

$$u_x^m = \frac{\beta gA}{\omega}\frac{ch\beta(z+d)}{ch\,\beta d}\cos(\beta x - \omega t) + \frac{3\omega\beta A^2}{8}\frac{ch2\beta(z+d)}{sh^4\,\beta d}\cos 2(\beta x - \omega t) + U_c \qquad (8)$$

$$u_y^m = \frac{\beta gA}{\omega}\frac{sh\beta(z+d)}{ch\,\beta d}\sin(\beta x - \omega t) + \frac{3\omega\beta A^2}{8}\frac{sh2\beta(z+d)}{sh^4\,\beta d}\cos 2(\beta x - \omega t) \qquad (9)$$

where A , ω , β , and d are wave amplitude, frequency, wave number, and water depth, respectively. x is the distance from origin to the wave making point. U_c is the current speed. A ramp function is used to smooth the transition from the start, $\phi_m = \phi t/T$, $t \leq T$, T is the wave period.

At the outlet, the pressure and turbulence quantities are also specified as zero normal gradients and the velocity is specified by Summerfield radiation condition. At the surfaces of structure, no slip wall boundary condition is used. The velocity vector at the bed is set to be zero and the zero normal gradient condition is chosen for other quantities. The bottom boundary of the domain is the bed. No slip wall boundary condition and wall function are used. For the atmosphere boundary, the total pressure is set to zero and k and ε are set to zero normal gradient.

In order to absorb the wave energy reflection from end-wall and re-reflection from input boundary, artificial damping zones are located at the two ends of domain. In present paper, for the right end damping zone in vertical direction, $D_i u_i$ damping term is added to the momentum equation. D_i is expressed as

$$D_i = \theta_i \sqrt{\frac{g}{h}}(n+1)\left(\frac{x-x_0}{l}\right)^n \qquad (10)$$

where l is the length of damping zone, x_0 is the distance from origin to the starting point of damping zone. n and θ_i are the damping coefficients, $n = 2$, $\theta_i = 0.6$. In horizontal direction along x, in order to keep the water level during the calculating time, $u_m = \bar{u} + (u - \bar{u})/D_1$ is applied at the every time step end, $\bar{u}$ is the mean velocity of last calculated period, u_m is the modified velocity. For the left damping zone, it is also a wave making region and the velocity in this area is modified by $u_i = u_i^m + D_i'(u_i - u_i^m)$ at the end of each time step. D_i' is written as

$$D_i' = \sqrt{1 - \left(\frac{l - x}{l}\right)^2} \tag{11}$$

1.3. Numerical implementation

The equations are discretized based on the FVM. In order to guarantee computational precision, the central difference scheme with second-order accuracy and Quadratic Upwind Interpolation of Convective Kinematics (QUICK) scheme with third-order accuracy are employed to represent the diffusion term and convection term respectively. The preconditioning conjugate gradient (PCG) method is employed for solving the algebraic equations. For solving the Navier-Stokes equation of incompressible fluid flow, there is a problem about the pressure-velocity coupling. Here, the PISO scheme is employed to treat the coupling. k and ε equations are coupled in the scheme and solved by a segregated approach. When the fluid domain is solved, the time history of wave force on the bodies can be obtained by integrating the pressure and viscous force. For free surface simulation, generally, it is easily involved calculation divergence because of the sharp interface between water and air. In this work, a compressive interface capturing scheme (CICSAM) is used to capture the fluid interfaces on mashes of arbitrary topology.

1.4. Drag and inertia coefficients

Chaplin [7] found that a good agreement between measured and computed forces could be obtained by separating hydrodynamic coefficients for the vertical and horizontal directions. In this work, the Morison's equation is modified and the forces for per unit length of the horizontally submerged circular cylinder can be write as

$$F_x = \frac{1}{2}\rho C_{DX} Ru\sqrt{u^2 + w^2} + \rho C_{MX} S\dot{u} \tag{12}$$

$$F_y = \frac{1}{2}\rho C_{DY} Rw\sqrt{u^2 + w^2} + \rho C_{MY} S\dot{w} \tag{13}$$

where F_x and F_y are the wave force in the horizontal and vertical direction respectively, ρ is the density, C_{DX} and C_{DY} are the drag coefficient in the horizontal and vertical direction respectively, C_{MX} and C_{MY} are the inertia coefficient in the horizontal and vertical direction respectively. u is the horizontal particle velocity and $\dot{u}$ is the horizontal particle acceleration. w is the vertical particle velocity and $\dot{w}$ is the vertical particle acceleration. R is the diameter of circular cylinder and S is the cross-sectional area of the cylinder.

In addition, the Morison's equation can be modified to account for the cases in wave-current flow, which can be expressed as

$$F_x = \frac{1}{2}\rho C_{DX} R(u + U_c)\sqrt{(u + U_c)^2 + w^2} + \rho C_{MX} S\dot{u} \tag{14}$$

$$F_y = \frac{1}{2}\rho C_{DY} Rw\sqrt{(u+U_c)^2 + w^2} + \rho C_{MY} S\dot{w} \qquad (15)$$

In this paper, the least-squares method is used to estimate the hydrodynamic coefficients. Using this method, based on force-time histories computed by present numerical method and modified Morison's equations, constant values of drag and inertia coefficients can be obtained. The C_D and C_M values are presented against KC number and the number can be defined as

$$KC = \frac{U_{max}T}{R} \qquad (16)$$

where U_{max} is the maximum horizontal particle velocity at the elevation of the centre of the cylinder section.

2. Numerical results and discussions

2.1. Model validation

Firstly, we investigate the characteristics of flow field in numerical wave-current tank. Two different experiment cases (wc2 and wc11) reported by Van Rijn [8] are used for evaluation of accuracy of the present numerical results. When the calculation becomes stably, the mean water level usually keeps unchanged. The calculated vertical distributions of time-average velocity are compared with experimental data in Fig. 2. The simulated results agree well with the experimental data. It is showed that the two-dimensional wave-current numerical tank has a good characteristic of wave-current combined flow.
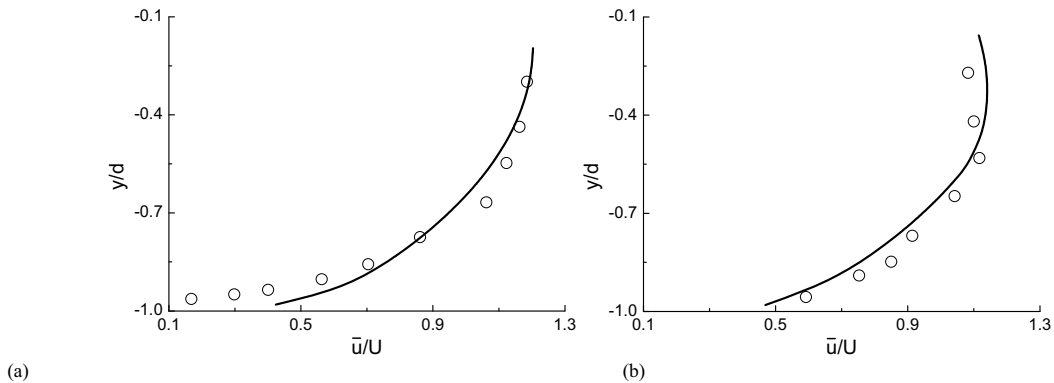

Fig. 2. Comparison of vertical distributions of time-average velocity (a) Wc2; (b) Wc11

Secondly, for the verification of the simulated wave forces, the calculation results are compared with Nojiri [9], Maruo [10], and Koo [5], respectively. A surface-piercing body is fixed in the middle of the domain and radius of round corner is 0.064 m. The incident wave height is 0.07 m. In order to capture the wave surface accurately and calculate the wave forces precisely. The meshes in surface zones and zones along body are refined. Fig. 3 shows the comparison of normalized drift force with Nojiri's experimental, Maruo's analytical and Koo's numerical results, where Fd is the drift force, $\xi = (B\omega^2)/(2g)$, ω is the wave frequency and B is the width of fixed cylinder, H is wave height. The computational results are shown to be in good agreement with experimental and numerical results of other researchers.
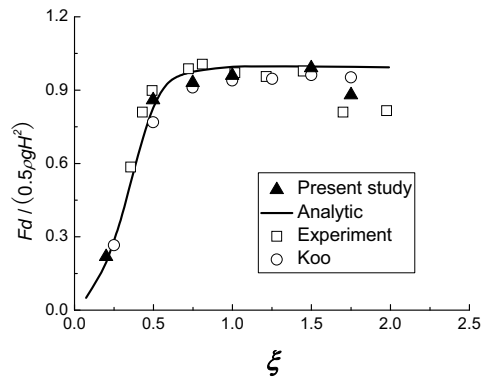
Fig. 3. Comparison of normalized drift force

2.2. Drag and inertia coefficients under waves

The calculated drag and inertia coefficients under waves are compared with the results of experiments. The experiments were carried out in the towing tank by Arai [11] and Venugopal et al. [3]. The dimensions of the tank used by Venugopal et al. [3] are 4.6 m wide, 2.7 m deep and 77 m long, with a working water depth of 2.2 m. The dimensions of test rectangular cylinder are 0.2 m breadth and 0.4 m width. For the model verification, one depth of submergence is chosen here, h=0.82 m. The drag and inertia coefficients for the submerged horizontal rectangular cylinder in waves are presented against KC number in Fig 4 and 5. The drag coefficients in present study are found to be lower than those reported by Venugopal but similar to those reported by Arai and a good comparison exists for inertia coefficients.
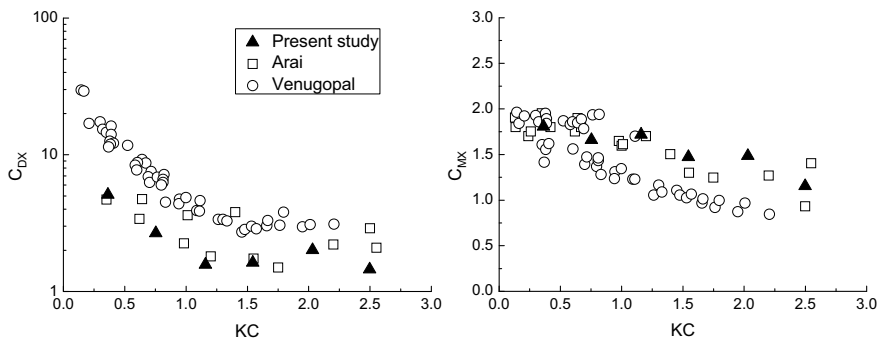

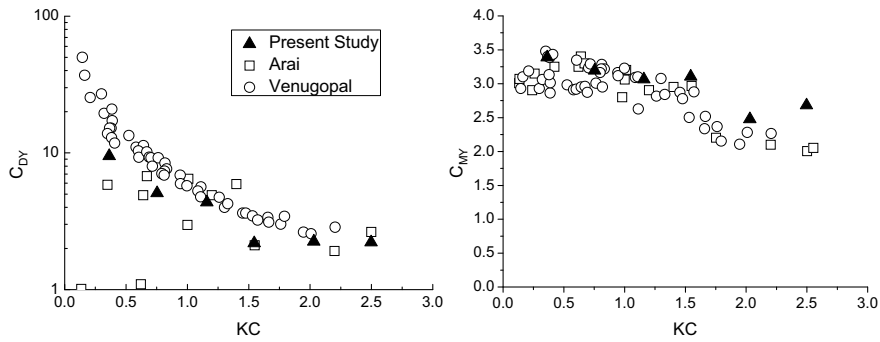Fig. 4. Horizontal drag and inertia coefficients for rectangular cylinder in waves

Fig. 5. Vertical drag and inertia coefficients for rectangular cylinder in waves

In Fig. 6 and Fig. 7, the drag and inertia coefficients for the submerged horizontal circular cylinder in waves are illustrated. The drag coefficients decrease significantly with increase in KC for both directions, while the inertia coefficients decrease slightly with increase of KC. At small KC numbers, the values of C_D and C_M for circular cylinders are obviously lower than those for rectangular cylinder. This phenomenon was also reported by Koterayama and Hu [12].
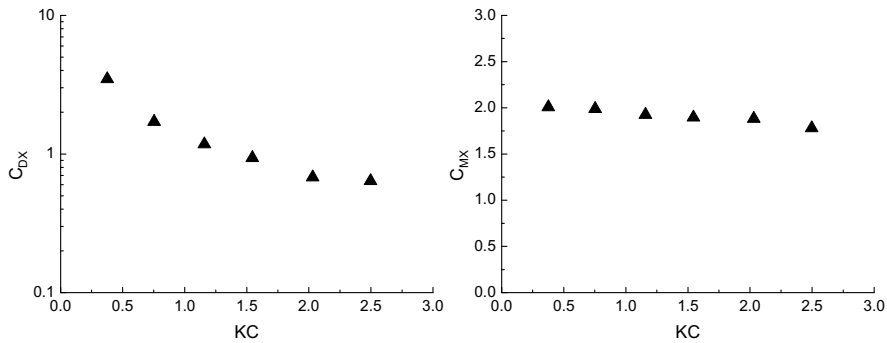

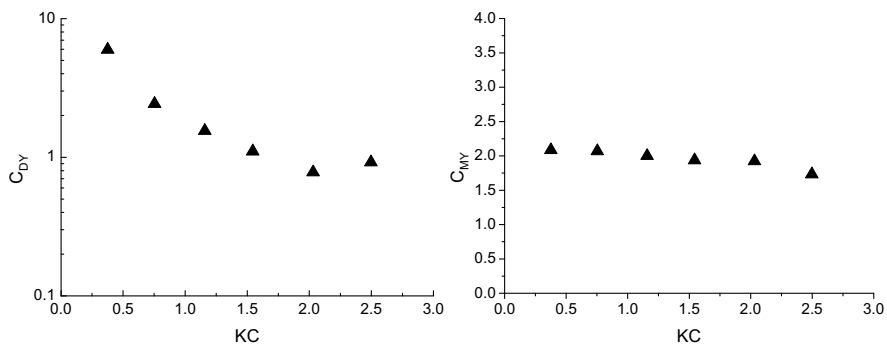Fig. 6. Horizontal drag and inertia coefficients for circular cylinder in waves

Fig. 7. Vertical drag and inertia coefficients for circular cylinder in waves

2.3. Drag and inertia coefficients under waves and currents

The drag and inertia coefficients for the submerged horizontal circular cylinder in currents are showed in Figs. 8 and 9, repotted along with the results in waves (Uc=0.0m/s). The figures indicate that the drag coefficients in horizontal direction in currents (Uc=0.1m/s) are significantly larger than the drag coefficients obtained in waves, especially for vertical drag coefficients. The horizontal and vertical inertia coefficients induced by wave-current flows in Fig 8 and 9 are found to be similar to those obtained in waves.
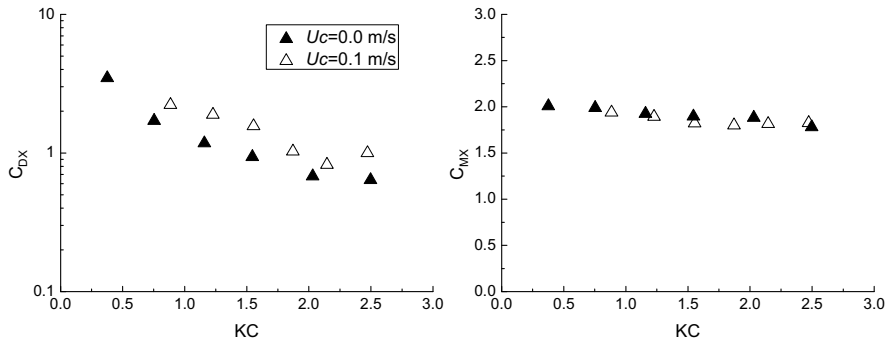

Fig. 8. Horizontal drag and inertia coefficients for circular cylinder in currents
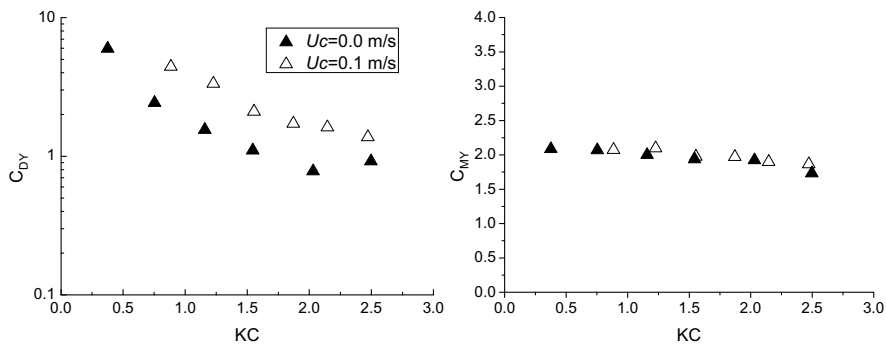

Fig. 9. Vertical drag and inertia coefficients for circular cylinder in currents

3. Conclusion

Based on the Reynolds averaged Navier-Stokes equations equations, a two-dimensional numerical wave-current tank is developed to compute the hydrodynamic forces and coefficients induced by waves and currents on submerged circular cylinder.

The computational vertical distributions of time-average velocity agree well with the experimental data and drift forces are also shown to be in good agreement with experimental and numerical results of other researchers. The verification indicates that the wave-current numerical tank has a good characteristic of wave-current combined flow and can be used to simulate the hydrodynamic forces on structures induced by waves and currents.

Simulated wave forces are then used to derive drag and inertia coefficients. The drag coefficients decrease significantly with increase in KC for both directions, while the inertia coefficients decrease slightly with increase of KC. In addition, the coefficients induced by waves and wave-current flows are compared. The results indicate that

the currents have a significant influence on the drag coefficients for submerged circular cylinder, while the vertical inertia coefficients induced by wave-current flows are found to be similar to those obtained in waves.

Acknowledgements

References

[1] Vinje T, Brevig P. Numerical simulation of breaking wave. *Proceedings of the Third International Conference on Finite Elements in Water Resources*, University of Mississippi, Oxford, 1981, 5: 196-210.

[2] Clement AH, Mas S. Hydrodynamic forces induced by solitary wave on a submerged circular cylinder. *Proceedings of the Fifth International Offshore and Polar Engineering Conference*, ISOPE, The Hague, 1995; 3: 339-347.

[3] Venugopal V, Varyani KS, Barltrop NDP. Wave force coefficients for horizontally submerged rectangular cylinders. *Ocean Engng* 2006; 33(11–12): 1669–1704.

[4] Venugopal V, Varyani KS, Westlake PC. Drag and inertia coefficients for horizontally submerged rectangular cylinders in waves and currents. *J. Engineering for the Maritime Environment* 2009; 223: 121-136.

[5] Koo WC, Kim MH. Fully nonlinear wave-body interactions with surface-piercing bodies. *Ocean Engineering* 2007; 34: 1000-1012.

[6] Dong Z, Zhan JM. Comparison of existing methods for wave generating and absorbing in VOF-based numerical tank. *Journal of Hydrodinamics* 2009; 24(1): 15-21.

[7] Chaplin JR. Loading on a cylinder in uniform oscillatory flow: Part II – elliptical orbital flow. *Appl. Ocean Res* 1988; 104: 199-206.

[8] Van Rijn LC. Data Base: sand concentration profiles and sand transport for currents and/or waves. Netherlands, Delft University of Technology, *Delft Hydraulics Report* H1148-04/05, 1991.

[9] Nojiri N, Murayama K. A study on the drift force on two-dimensional floating body in regular waves. *Transactions of the West-Japan Society Naval Architect* 1975; 51: 131-152.

[10]Maruo H. On the increase of the resistance of a ship in rough seas. *Journal of Zosen Kiokai* 1960; 108.

[11]Arai S. Forces and circulation of horizontal cylinders submerged in regular waves. In: *Proceedings of the Third International Offshore and Polar Engineering Conference*, Singapore, 1993 3: 288-293.

[12]Koterayama W, Hu C. Wave forces on horizontal cylinders at low Keulegan–Carpenter and Reynolds numbers. *Proceedings of the Fifth International Offshore and Polar Engineering Conference*, The Hague, The Netherlands, 1995: 189-195.